3.6.4

^{3}He-free triple GEM thermal neutron detectors

A. Pietropaolo[1,2], G. Claps[1], F. Murtas[3], L. Quintieri[4], G. Celentano[1], A. Vannozzi[1],A. Santoni[1] R. Riedel[5]

1 ENEA Frascati Research Center, via E. Fermi 45, 00044 Frascati (Roma), Italy
2 MIFP, Mediterranean Institute of Fundamental Physics - Via Appia Nuova 31, 00040 Marino (Rome), Italy
3 CERN, CH-1211 Geneva 23, Switzerland
4 ENEA Casaccia Research Center, via Anguillarese 301, 00123 S. Maria di Galeria (Rome), Italy
5 Oak Ridge National Laboratory - 2008 MS-6466, Oak Ridge, TN 37831-6466, USA

***Corresponding author**: antonino.pietropaolo@enea.it

Abstract. A novel type of thermal neutron detector based on the gas electron multiplier (GEM) technology is presented in the framework of the research and development activity on the ^{3}He replacement for neutron detection. The device relies on a series of boron-coated alumina sheets placed perpendicularly to the incident neutron beam direction. The detector, named side-on GEM (S-GEM), was tested (in a prototypal version) on beam at the TRIGA reactor of the ENEA-Casaccia Research Centre (Italy), ISIS spallation neutron source (UK) and at the High Flux Isotope Reactor at the Oak Ridge National Laboratory (US) to assess its performance. The obtained results demonstrate the effectiveness of the proposed detector configuration to achieve a good spatial resolution and, in the perspective, higher thermal neutron efficiency, comparable to ^{3}He tubes typically used for diagnostic in nuclear reactors. The main issues to be addressed to reach the goal, mostly related to boron coating procedures and characterization, are also pointed out.

1. Introduction

The global shortage of ^{3}He for neutron detection purposes triggered an intense and interesting research and development activity worldwide to find out effective solutions. Different approaches have been proposed so far such as the use of boron or lithium fluoride loaded detectors [1–6]. Although reactions producing charged particles in the final state are widely investigated, also thermal neutron radiative capture has been recently used [5,7,8]. In this paper, a particular gaseous detector, namely the gas electron multiplier (GEM) [9], is described. In particular, a triple GEM device [10,11] was equipped with a sequence of alumina sheets, coated by boron films on both wide surfaces, acting as neutron–charged-particle converters. The detector window is made on the frames of the GEM foils, so that the neutron beam can impinge laterally (that is, perpendicularly to the wider surface) onto the detector rather than frontally, as typically happens in other applications [12,13]. The device, conceived and assembled at the Istituto Nazionale di Fisica Nucleare (INFN-Laboratori Nazionali di Frascati) and named as side-on GEM (S-GEM) [14], was tested at the TRIGA reactor (ENEA-Casaccia Research

Centre, Italy), ISIS spallation source (UK) and High Flux Isotope Reactor (HFIR) (Oak Ridge National Laboratory, US) [15,16]. Previously to experimental tests, a series of Monte Carlo simulations, thoroughly described and discussed in Ref. [14] were performed using two different codes for a thorough description of the physics underlying the detector's operation and as a mandatory validation step for other simulations of more complex detector's architectures that should lead to define a more efficient device.

2. Experimental setups and measurements

The S-GEM detector structure is shown in figures 1 and 2.

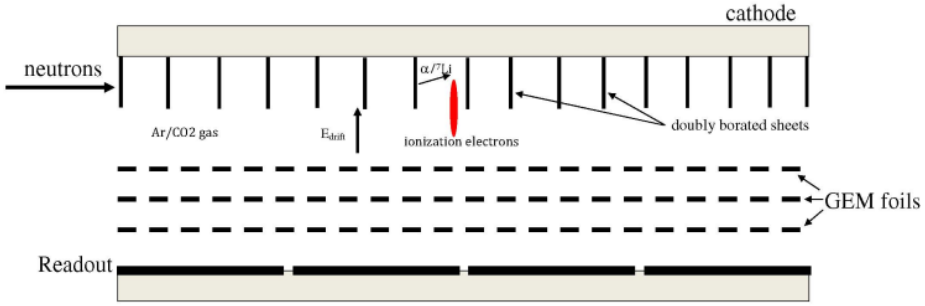

Figure 1: *Schematic of a S-GEM detector*

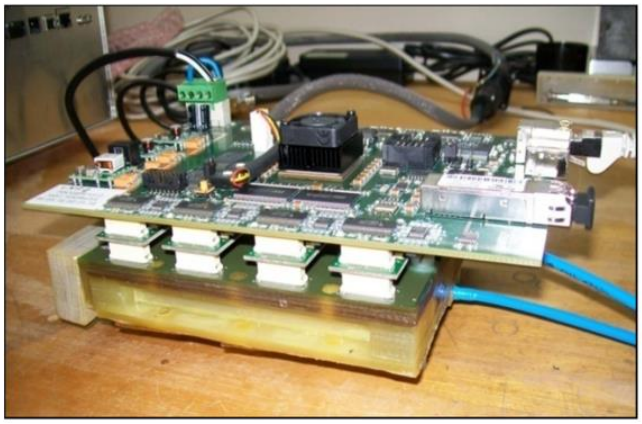

Figure 2: *Picture of an assembled S-GEM*

In the S-GEM configuration, the neutron beam impinges perpendicularly to the wider alumina sheets, that is parallel (rather than perpendicular) to the cathode contrarily to the typical configuration applied in almost all GEM-based detectors applications. When a neutron is absorbed in the ^{10}B layer, an alpha particle and a ^{7}Li ion are produced following the reactions $n+^{10}B \rightarrow ^{4}He+^{7}Li$ (Q=2.8 MeV, BR=7%) or $n+^{10}B \rightarrow ^{4}He+^{7}Li+\gamma$(478 keV) (Q=2.3 MeV, BR=93%). The secondary ions ionize the Ar/CO_2 gas mixture (70%/30%) in the drift region of the detector thus producing electrons that, moving under the influence of the electric field in this region, reach the three GEM foils. In this region they are further proportionally multiplied in cascade, inducing a detectable signal in the pad-based readout. The first S-GEM prototype designed was made of two sets of five 40x10x1 mm^3 glass sheets arranged in the same detector: a borated set and not borated one in order to check, under localized irradiation, the difference between the two sets (the reader is referred to Ref [14] for more details). The readout was composed of 128 pads 3x6 mm^2 organized in a matrix of 16x8. ^{10}B coating was obtained by means of electron beam evaporation techniques. Located on the external side, there is the readout electronics consisting of a set of eight CARIOCA chip cards and a FPGA mother board, the details being described in ref. [12].

The upgraded version of the S-GEM was made with the readout pads arrangement chosen in such a way to achieve a better spatial resolution along the beam direction. The cathode is an aluminium plate, that on the internal side facing the gas mounts 16 borated alumina sheets in half of the active volume of the drift region and one borated alumina sheet on the other half side. Each sheet is 50 mm long, 10 mm high and 400 μm thick while the drift region is 12 mm high, so that the sheets do not touch the first GEM foil. A 10×1 cm^2 area 0.5 mm thickness of epoxy glass window was obtained on the lateral side of the drift region and parallel to the borated sheets.
Both the detectors film depositions were carried out at the ENEA-Frascati Research Centre (Italy) using a vacuum chamber equipped with a multi-crucible Thermionics 3 kW electron beam system with 4 kV of electron acceleration voltage and 750 mA of maximum current. Boron tablets of 0.5 inches diameter were used as source for evaporation using boron metal powder enriched in ^{10}B (isotopic ^{10}B > 97 at%, Eagle Picher Technologies, LLc). Five glass substrates were disposed side by side on a rotating sample holder in such a way that both surfaces could be subsequently exposed to the evaporation source and substrates could be completely coated during the same coating process. Film growth rate was monitored by a quartz crystal controller and fixed at 0.2–0.3 nm/s by tuning the electron beam current. The distance between the evaporation source and sample holder was 12.5 cm. In this configuration, the film thickness uniformity over the whole deposition area 40x50 mm^2 is greater than 90%. Each surface was coated with 300 nm ^{10}B film. Although the optimized thickness may be in the order of about 1 μm, this thickness was chosen to achieve a low intrinsic efficiency for a single sheet, as the detector was to be used on the direct neutron beam in a condition similar to a beam monitor. Films as thick as 680 nm were successfully deposited on a single surface exhibiting good adherence and stability against aging (no delamination occurred within 2–3 months).

2.1 TRIGA measurements

The first prototype S-GEM with glass sheets was tested at the TRIGA reactor operating at the ENEA-Casaccia Research Centre (Italy) [17]. The reactor can be operated at different powers, from a few Watt to 1 MW, with a neutron flux of about 2x10^6 n/cm^2/s (at the maximum power) featuring a Maxwellian spectrum peaked 25 meV and a FWHM of about 70 meV, as shown in figure 3.

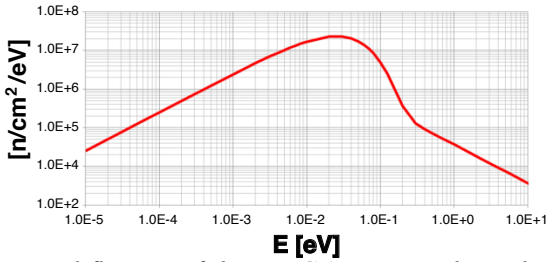

Figure 3: *Neutrons spectral fluence of the TRIGA reactor along the thermal extraction line*

By running at different powers (and thus at different neutron fluxes) the detector response was investigated in terms of detector's count rate as a function of the incident neutron rate from the beam line. Figure 4 shows S-GEM counts and reactor power (from a few Watt to 1 MW) as a function of time and the correlation between the S-GEM count rate and the neutrons rate provided by the reactor along the extraction port chosen for the measurements. A good linearity over 6 orders of magnitude is found and the slope of the fitting line, that provides an estimation of the detection efficiency, results to be 4.8(5)%.

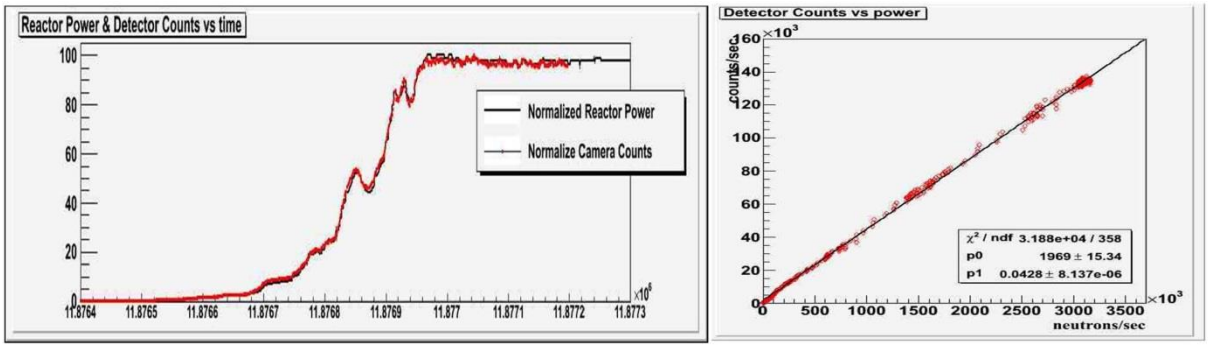

Figure 4: *(left) Normalized S-GEM counts (red) and TRIGA power (black) as a function of time; (right) S-GEM counts vs neutron rate (correlation plot). The linear fit provides detector's efficiency.*

2.2 ISIS measurements

The same detector tested at the TRIGA reactor was also tested at the ISIS spallation neutron source [18] at the Rutherford Appleton Laboratory (UK) using the ROTAX beam line [19]. This instrument is a neutron diffractometer, mostly used for magnetic neutron scattering and cultural heritages studies using neutron diffraction [20,21]. At present, it is used as a test beam line for detector development [22,23]. ROTAX is downstream of the PRISMA beam line and it is in the line of view of a solid methane moderator at T~95 K. The primary flight path (from moderator to the sample position) is $L_0 \approx 15$ m. A T0 chopper blocks the beam when the protons hit the target thus blocking out a large component of the fast neutrons and gammas, while the use of the neutron guides in the front end of the PRISMA beam line ensures an enhanced thermal neutron intensity at the sample position. The neutron spectrum is peaked at about 10 meV and features a high energy tail up to multi-MeV energies [24]. The measurement was performed by placing the S-GEM in the incident neutron beam at a distance of about 16 m from the moderator and recording neutron counts by using a time window of 1 ms and delaying it with respect to the ISIS clock in steps of 1 ms from 0 to 19 ms (i.e. the whole time frame of ISIS beam lines). The detector was biased at a voltage of about 870 V, that is at a gain to ensure an almost complete rejection of the gamma background (see figure 5 and refer to Ref. [11]), composed of different contributions and always occurring in a neutron beam line and [25,26].

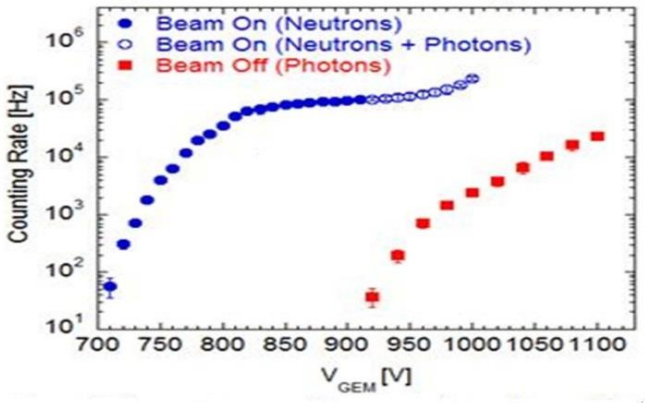

Figure 5: *S-GEM counting rate as a function of total GEM bias for different irradiation conditions*

The detector results insensitive to the 478 keV gamma rays coming from the radiative thermal neutron capture in boron. The reconstructed time spectrum (corresponding to the incident neutron spectrum in the time-of-flight domain) is shown in Fig. 6 and compared to the same spectrum measured by the ROTAX incident neutron beam monitor (a Li-glass scintillation detector) operating with the standard

Data Acquisition Electronics used at ISIS. The two spectra were normalized with respect to the peak at 6 ms of the S-GEM spectrum for a more clear shape comparison. The two trends are very similar and show a peak at about 6 ms and then a rapid falling edge starting at 2 ms. The peak at 6 ms is the peak of the Maxwell–Boltzmann component of the neutron spectrum induced by the effect of the moderator while the rapid decrease below 2 ms is due to the combined effect of the T0 chopper operating on ROTAX, and used to cut away from the beam the high-energy neutrons components and the gamma flash from the target, and the decreasing efficiency of the monitor and S_GEM with increasing neutron velocity (both ^{6}Li and ^{10}B absorption cross section decrease as 1/v, v being the neutron velocity).

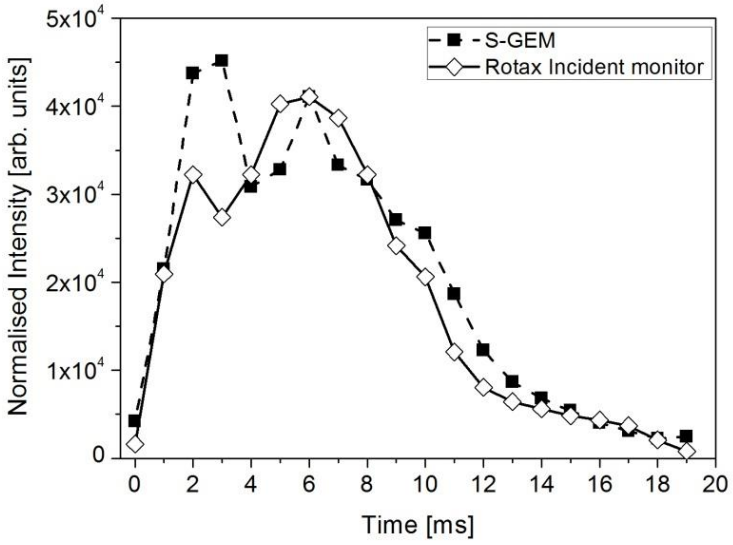

Figure 6: *Comparison between the time of flight neutron spectrum recorded by the Li-glass neutron beam monitor of ROTAX and that recorded by the S-GEM (see text for details).*

Another measurement was performed on ROTAX by placing two close spaced (about 5 mm distance) cadmium sheets, 1 mm thickness and about 10x1 cm^2 area. The two sheets were placed in front of the entrance window of the S-GEM in such a way to intercept the incident neutron beam and absorb thermal neutrons impinging onto the Cd surface. Indeed, 1 mm natural Cd provides a very high (close to 100%) absorption efficiency for neutrons with energy up to about 400 meV (cadmium cut-off). Figure 7 shows the 2D intensity plots and the corresponding contour plots relative to the measurements with and without the cadmium sheets in front of the S-GEM. In the right panel, counts are registered in the region between the two absorbing Cd sheets. It is to be stressed that in both cases shown in Fig. 7, the signals from gamma-rays (both environmental as well as from neutron radiative capture in ^{10}B and Cd) do not contribute thanks to the high rejection capability of the detector at the used operational bias. This further measurement is a clear demonstration that the S-GEM detector is sensitive to thermal neutron with a spatial resolution related to the pad's dimension.

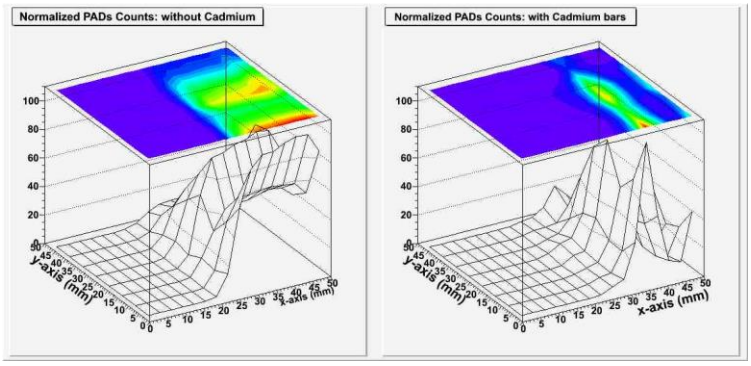

Figure 7: *2D Intensity profiles recorded through the S-GEM, obtained by using two cadmium sheets in front of the detector*

2.3 HFIR measurements

The S-GEM detector mounting 16 borated alumina sheets was characterized at the CG1A beam line at the HFIR facility, a nuclear research reactor located at Oak Ridge National Laboratory (ORNL, Oak Ridge, Tennessee, US). HFIR operates at 85 MW power and is one of the highest-flux reactor-based sources of neutrons for condensed-matter research in the United States. CG1A is a detector test station providing 4.2 Å neutrons at an estimated flux of 2×10^6 n cm^{-2}. The neutron beam used for the measurements extended on an irradiation area of 5×5 cm^2 and had an angular divergence lower than one degree, making it extremely useful to characterize resolution, uniformity, distortion and performance with a high neutron flux. The HFIR neutron spectrum, shown in figure 8, features a Maxwell-Boltzmann distribution peaked at λ= 4.23 Å (E ~ 4.57 meV) with a Full Width at Half-Maximum (FWHM) of about 0.11 Å.

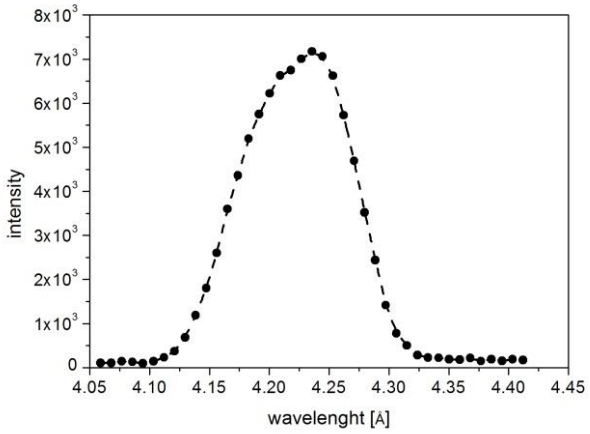

Figure 8: *HFIR neutron spectrum as a function of wavelength.*

This spectrum is measured using the time-of-flight analysis. This is accomplished by using a pinhole neutron chopper operating at about 100 Hz and a ^{3}He detector approximately 1.5 m from the chopper. The main goals of the experimental tests were to evaluate linearity and accuracy in beam positioning and to measure the detector efficiency. For beam intensity tests, the experimental set-up is sketched in figure 9.

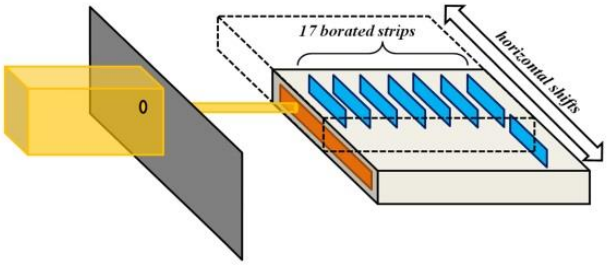

Figure 9: *Schematic of the experimental setup for the S-GEM measurements at HFIR reactor*

A 2 mm thick borated aluminium mask was placed at a distance of about 2m from the source to provide an almost complete absorption of about 99.7% neutrons over the whole spectrum shown in fig. 8. The mask features a 2.5 mm diameter hole to provide a collimated beam for positioning tests described below. Beyond the screen there was the S-GEM detector mounted on a mobile support so that it could be displaced along the horizontal direction parallel to the window. During the beam positioning tests the detector was moved in steps of 10 mm (with an accuracy of better than 10 μm) scanning in such a way the whole window by the small-hole beam. Then, to make efficiency measurements, an ^{3}He tube (1 cm in diameter and 30 cm long with 10 bar pressure) was placed in front of the S-GEM detector providing an efficiency close to 1 at the neutron spectrum peak. During the S-GEM measurements the ^{3}He detector was moved away, while during the measurements with the ^{3}He tube the GEM detector was not recorded. The S-GEM measurements were performed in two different positions with respect to the beam passing through the mask hole, in order to irradiate the 16-sheets region and the single-sheet one. To evaluate the overall background sensitivity of both ^{3}He and GEM detectors, the measurements were done also with the mask hole closed. The S-GEM was operated with a biasing voltage of 870V, corresponding to a gain of about 180, that allows an effective lowering of the gamma sensitivity as already shown in other experimental tests [11,14]. The ^{3}He tube used a PDT model 20A preamplifier and was biased at about 1200 V. The TTL output of the PDT preamplifier is input into an ORTEC 974 counter and the count rate is the average value over a 100 s counting time. The efficiency of the ^{3}He tube has been verified using a second ^{3}He tube operating under similar conditions with a different PZT amplifier. Dead time loss is not significant in the ^{3}He detector below 1E+4 counts s^{-1}. During the detector position scan, a sequence of 3D beam profiles like those shown in figure 10(a) was measured. The 2D beam profile [figure 10(b)] was obtained by summing all the counts on the four pads along the X-axis. A Gaussian function was used to fit these profiles: their central value provides a measure of the beam positions. Figure 10(c) shows the intensity profiles along the X-direction (neutron beam axis) for the four pads rows. The S-GEM detector worked using an internal trigger and registered the number of counts over a time window of 1 s after each trigger.

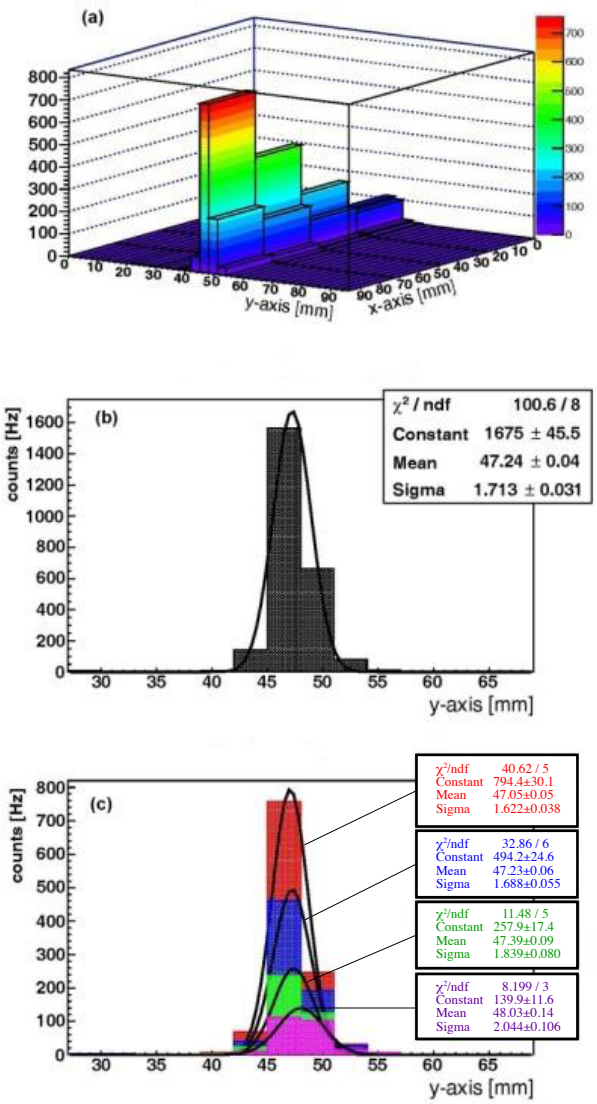

Figure 10: *(a) 3D beam profiles measured during the detector position scan over the active window; (b) a beam profile on the Y section, obtained summing all the counts on the pads along X-direction; (c) beam profiles obtained on the 32 Y pads on each of the four pads sectors along the X direction.*

The Gaussian fit shows an increase in the FWHM of the beam profile, along the neutron flight path inside the detector, of about 25% between the first and the last pads sector. This is most likely due to a small divergence of the beam. A position resolution of 770±80 μm is found [27]. In figure 11, the 3D plots represent the cumulative counts distribution on each pad obtained by summing the counts for each trigger. Analysing these distributions, it is possible to calculate the mean of the counts number and its uncertainty for the two beam configurations.

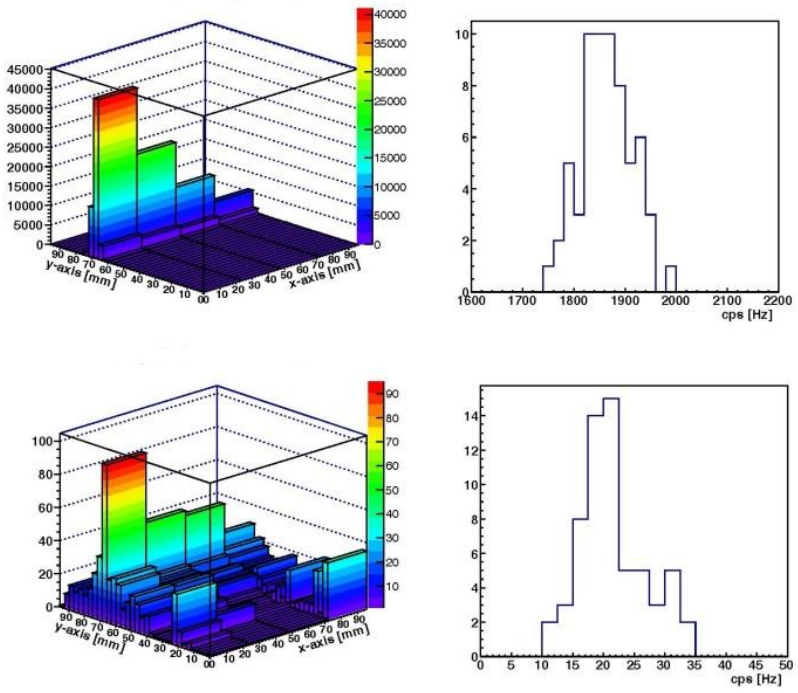

Figure 11: *(upper panel) 3D plot of the total counts distribution in the S-GEM in the open pencil beam configuration and histogram of the total counts distribution in the S-GEM, obtained summing over the whole set of acquisition triggers of the measurement. (Lower panel) the same kind of plots of the the upper panel but for the closed pencil beam configuration, i.e. background measurements.*

Table 1 reports the calculated values of the efficiency S/B ratio for S-GEM and ^{3}He tube. The background counts in the S-GEM are mostly due to environmental neutrons (almost an isotropic components and a directional one due to neutron beam, passing through the mask) as the gamma sensitivity at the chosen operation bias is almost null. The higher background sensitivity of the ^{3}He tube, as compared to the S-GEM, is primarily due to the incomplete shielding of 30 cm long tube to background neutrons. The absolute S-GEM efficiency was calculated as

$$\varepsilon_{\text{S-GEM}} = \frac{(C_{\text{GEM}} - C_{\text{GEM-BCKG}})/CS}{(C_{^3\text{He}} \cdot C_{^3\text{He-BCKG}})/\varepsilon_{^3\text{He}}} \quad (1)$$

In relation (1), C_{GEM} and $C_{\text{GEM-BCKG}}$ are the overall counts and the background counts in the S-GEM, respectively, while $C_{^3\text{He}}$ and $C_{^3\text{He-BCKG}}$ are the same quantities for the ^{3}He tube; $\varepsilon_{^3\text{He}}$ is the ^{3}He tube absolute efficiency (99%) and CS is the cluster size. This last value is a statistical parameter taking into account the possibility for a neutron to fire more than one single pad in the S-GEM detector. Estimation of cluster size has been obtained carrying out measurements with small integration times (< 20 μs) and very low intensity beams. The estimated value at 870 V is CS=1.34 ± 0.02. The evaluated absolute efficiency at 5.1 meV of the S-GEM on the 16-sheets region is 31% ± 1%, while for the single-sheet region it is found to be (2.8 ± 0.5)%.

Table 1: Signal and background counts for S-GEM and ^{3}He tube detectors and measured values of signal-to-background ratio and efficiency, the efficiency of ^{3}He tube being known by measurements performed previously

	S-GEM	**^{3}He Tube**
Overall mean counts [s^{-1}]	1863	6011
Background mean counts [s^{-1}]	21	1586
Signal/Background	87.7	2.8
Efficiency [%]	31	99
Single sheet efficiency [%]	2.8	

3. Conclusions and perspectives

A new configuration of a GEM-based neutron detector named Side-on GEM (S-GEM) was tested and characterized on beam at the TRIGA reactor (ENEA Casaccia), ISIS spallation neutron source (Rutherford Appleton Laboratory, UK) and the HFIR reactor (Oak Ridge National Laboratory, US), respectively. Two different prototypes were tested: a first detector made of a series of glass sheets borated on both sides, the ^{10}B layer being 300 nm, and filled by Ar/CO2 mixture, a second one with 16 alumina sheets borated with 1 μm ^{10}B. The tests at the TRIGA reactor provided a first experimental determination of the detector efficiency and of its dynamic range in the present configuration, over an extended interval of neutron flux. The experimental tests at ISIS showed the effectiveness of the S-GEM in detecting thermal neutrons, producing the main features of the neutron spectrum in a comparable way with respect to the standard neutron beam monitor used on the beam line. The HFIR tests have shown an improved efficiency and improved spatial resolution thanks to an optimized pads layout, also pointing out important issues to be addressed on boron deposition. In perspective, the devices can be made more efficient by a controlled deposition procedure and new tests are envisaged both on the reactors and time of flight neutron sources.

References

[1] Kouzes R. T., Ely J. H., Lintereur A. T., Siciliano E. R. and Woodring M. L., PNNL Report, No. 19050 (2009).
[2] Lintereur A., Conlin K., Ely J., Erikson L., Kouzes, R., Siciliano E., Stromswold D. and Woodring M., Nucl. Instrum. Methods A **652** (2011), 347.
[3] Klein M. and Schmidt C. J., Nucl. Instrum. Methods A **628** (2011) 9.
[4] Tremsin A. S., Feller W. B. and Downing R. G., Nucl. Instrum. Methods A **539** (2005), 278.
[5] Festa G., Pietropaolo A., Grazzi F., Barzagli E.,Scherillo A. and Schooneveld E. M., Nucl. Instrum. Methods A **654** (2011),373.
[6] Barbagallo M., Cosentino L., Greco G., Guardo, ., Montereali R. M., Pappalardo A., Scirè C., Scirè S., Vincenti M. A. and Finocchiaro P., Nucl. Instrum. Methods A **652** (2011), 355.
[7] Festa G., Pietropaolo A., Reali E., Grazzi F. and Schooneveld E. M., Meas. Sci. Technol., 21 (2010) 035901.
[8] Pietropaolo A. et al., in prepration.
[9] Sauli F., Nucl. Instrum. Methods A, 386 (1997) 531.
[10] Murtas F., Buonomo B., Corradi G., Mazzitelli, G., Pistilli M., Poli Lener M., Tagnani D. and Valente P.,Nucl. Instrum.Methods A, 617 (2010) 237.
[11] Murtas F., Croci G., Pietropaolo A., Claps G.,Frost C. D., Perelli Cippo E., Raspino D., Rebai M., Rhodes N. J., Schooneveld E. M., Tardocchi M. and Gorini G., JINST, 7 (2012) P07021.

[12] Bonivento W., Jarron P., Moraes D., Riegel W. and Dos Santos F., Nucl. Instrum. Methods A, 491 (2002) 233.
[13] Guedes G. P., Breskin A., Chechik R., Vartsky D., Bar D., Barbosa A. F. and Marinho P. R. B., Nucl. Instrum. Methods A, 513 (2003) 473.
[14] Pietropaolo A., Murtas F., Claps G., Quintieri L., Raspino D., Celentano G., Vannozzi A. and Frasciello O., Nucl. Instrum. Methods A, 729 (2013) 117.
[15] HFIR website: http://neutrons.ornl.gov/facilities/ HFIR/.
[16] Berry K. D., Bailey K. M., Beal J., Diawara Y., Funk L., Hicks J. S., Jones A. B., Littrell K. C., Pingali S. V., Summers P. R., Urban V. S., Vandergriff D. H., Johnson N. H. and Bradley B. J., Nucl. Instrum. Methods A, 693 (2012) 179
[17] ISIS web site: ⟨www.isis.stfc.ac.uk⟩.
[18] Tietze H., Schmidt W., Geick R., Physica B **156–157** (1989) 550 ⟨http://www.isis.stfc.ac.uk/instruments/rotax⟩.
[19] Kockelmann W., Kirfel A., Physica B 350 (2004) e581.
[20] Filabozzi A., Andreani C., De Pascale M.P.,. Gorini G, Pietropaolo A., Perelli Cippo E., Senesi R., Tardocchi M., Kockelmann W., Journal of Neutron Research **14** (2006), 55.
[21] Pietropaolo A., Andreani C., Rebai M., Giacomelli L., Gorini G., Perelli Cippo E., Tardocchi M., Fazzi A., Verona Rinati G., Verona C., Marinelli M., Milani E., Frost C.D., Schooneveld E.M., Europhys. Lett. **92** (2010), 68003.
[22] Pietropaolo A., Andreani C., Rebai M., Giacomelli L., Gorini G., Perelli Cippo E., Tardocchi M., Fazzi A., Verona Rinati G., Verona C., Marinelli M., Milani E., Frost C.D., Schooneveld E.M.,Europhys. Lett.**94** (2011), 62001.
[23] Bedogni R., Esposito A., Andreani C., Senesi R., De Pascale M.P., Picozza P., Pietropaolo A., Gorini G.,. Frost C.D, Ansell S., Nucl. Instr. Meth. A **612** (2009) 143.
[24] Smirnov A.N., Pietropaolo A., Prokofiev A.V., Rodionova E.E., Frost C.D., Ansell S., Schooneveld E.M., Gorini G., Nucl. Instr. Meth. A **687** (2012), 14.
[25] Pietropaolo A., Tardocchi M., Schooneveld E.M., Senesi R., Nucl. Instr. Meth. A **568** (2006), 826.
[26] Pietropaolo A., Perelli Cippo E., Gorini G., Tardocchi M., Schooneveld E.M., Andreani C., Senesi R., Nucl. Instr. Meth. A **608** (2009), 121.
[27] Claps G., Murtas F., Pietropaolo A., Celentano G., Vannozzi A., Santoni A.,. Quintieri L and Riedel R. A., Europhys. Lett. **105** (2014), 22002.